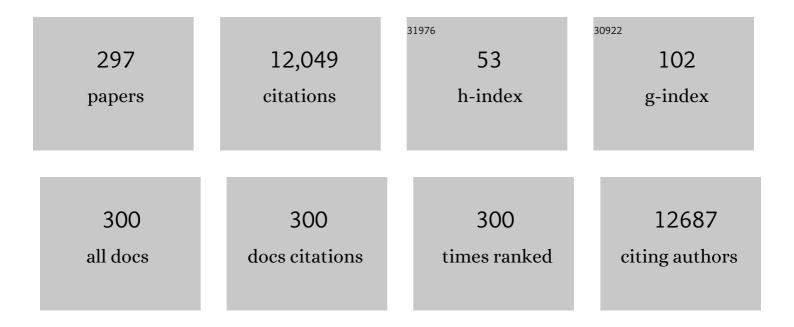
Tian-Ling Ren

List of Publications by Year in descending order

Source: https://exaly.com/author-pdf/4283062/publications.pdf Version: 2024-02-01



#	Article	IF	CITATIONS
1	Recent progress of continuous intraocular pressure monitoring. Nano Select, 2022, 3, 1-19.	3.7	4
2	Highly stretchable and conformal electromagnetic interference shielding armor with strain sensing ability. Chemical Engineering Journal, 2022, 431, 133908.	12.7	15
3	Industrial-scale production of high-quality graphene sheets by millstone grinders. Journal Physics D: Applied Physics, 2022, 55, 164002.	2.8	2
4	An intelligent nanomesh-reinforced graphene pressure sensor with an ultra large linear range. Journal of Materials Chemistry A, 2022, 10, 4858-4869.	10.3	14
5	Highâ€Throughput DNA Tensioner Platform for Interrogating Mechanical Heterogeneity of Single Living Cells. Small, 2022, 18, e2106196.	10.0	15
6	Impact of Molybdenum Oxide Electrode on the Ferroelectricity of Doped-Hafnia Oxide Capacitors. IEEE Transactions on Electron Devices, 2022, 69, 1492-1496.	3.0	8
7	Review on Organic–Inorganic Two-Dimensional Perovskite-Based Optoelectronic Devices. ACS Applied Electronic Materials, 2022, 4, 547-567.	4.3	35
8	Intelligent and highly sensitive strain sensor based on indium tin oxide micromesh with a high crack density. Nanoscale, 2022, 14, 4234-4243.	5.6	6
9	Mini-review: Novel Graphene-based Acoustic Devices. Sensors and Actuators Reports, 2022, 4, 100086.	4.4	2
10	Intelligent and Multifunctional Graphene Nanomesh Electronic Skin with High Comfort. Small, 2022, 18, e2104810.	10.0	42
11	A Better Zn-Ion Storage Device: Recent Progress for Zn-Ion Hybrid Supercapacitors. Nano-Micro Letters, 2022, 14, 64.	27.0	65
12	Humidity-Based Human–Machine Interaction System for Healthcare Applications. ACS Applied Materials & Interfaces, 2022, 14, 12606-12616.	8.0	22
13	Vertical MoS2 transistors with sub-1-nm gate lengths. Nature, 2022, 603, 259-264.	27.8	251
14	Electrooculography and Tactile Perception Collaborative Interface for 3D Human–Machine Interaction. ACS Nano, 2022, 16, 6687-6699.	14.6	44
15	Skinâ€Mimicking, Stretchable Photodetector for Skin ustomized Ultraviolet Dosimetry. Advanced Materials Technologies, 2022, 7, .	5.8	6
16	Two-stage amplification of an ultrasensitive MXene-based intelligent artificial eardrum. Science Advances, 2022, 8, eabn2156.	10.3	62
17	Exploration of the Mass Sensitivity of Quartz Crystal Microbalance under Overtone Modes Using Electrodeposition Method. Analytical Chemistry, 2022, 94, 5760-5768.	6.5	2
18	Nomex paper-based double-sided laser-induced graphene for multifunctional human-machine interfaces. Carbon, 2022, 193, 68-76.	10.3	13

#	Article	IF	CITATIONS
19	Ultrathin encapsulated rGO strain sensor for gesture recognition. Microelectronic Engineering, 2022, 259, 111779.	2.4	10
20	Biocompatible Sensors Are Revolutionizing Healthcare Technologies. , 2022, , 227-249.		1
21	Ultra-Low Voltage Schmitt Triggers Implemented by HfO ₂ -Based Ferroelectric Field-Effect Transistors. IEEE Electron Device Letters, 2022, 43, 1145-1148.	3.9	1
22	Graphene-Based Flexible Electrode for Electrocardiogram Signal Monitoring. Applied Sciences (Switzerland), 2022, 12, 4526.	2.5	12
23	Electrospun Nanofibers for Integrated Sensing, Storage, and Computing Applications. Applied Sciences (Switzerland), 2022, 12, 4370.	2.5	6
24	Deep Learning Enabled High-Performance Speech Command Recognition on Graphene Flexible Microphones. ACS Applied Electronic Materials, 2022, 4, 2306-2312.	4.3	5
25	The Trend of 2D Transistors toward Integrated Circuits: Scaling Down and New Mechanisms. Advanced Materials, 2022, 34, e2201916.	21.0	37
26	Quasi-Fermi-Level Phase Space and its Applications in Ambipolar Two-Dimensional Field-Effect Transistors. Physical Review Applied, 2022, 17, .	3.8	2
27	Wafer-Scale Photolithography-Pixeled Pb-Free Perovskite X-ray Detectors. ACS Nano, 2022, 16, 10199-10208.	14.6	25
28	Cs ₂ AgBiBr ₆ -Tellurium heterojunction-based high-performance X-ray detectors. , 2022, , .		1
29	A Low-cost, Low-power, and Practical Nano-heterojunction Pollution Gas Sensor Based on Accurate Dielectrophoresis Technology. , 2022, , .		Ο
30	Electromyogram-strain synergetic intelligent artificial throat. Chemical Engineering Journal, 2022, 449, 137741.	12.7	11
31	Light-Controlled Reconfigurable Optical Synapse Based on Carbon Nanotubes/2D Perovskite Heterostructure for Image Recognition. ACS Applied Materials & Interfaces, 2022, 14, 28221-28229.	8.0	6
32	A Flexible Graphene-Based Fabric Ultrasound Source for Machine Learning Enhanced Information Encryption. IEEE Electron Device Letters, 2022, 43, 1543-1546.	3.9	4
33	The α-In ₂ Se ₃ THz Photodetector. IEEE Transactions on Electron Devices, 2022, 69, 4371-4376.	3.0	1
34	Investigation of Q Factor of the QCM Resonator Under Overtone Modes. , 2022, , .		0
35	Stability diagrams of two optically mutual-injected quantum cascade lasers. AIP Advances, 2021, 11, 015320.	1.3	0
36	A Shoe-Integrated Sensor System for Long- Term Center of Pressure Evaluation. IEEE Sensors Journal, 2021, 21, 27037-27044.	4.7	10

#	Article	IF	CITATIONS
37	Enhancing the Ultraviolet Photocurrent and Response Speed of Zinc Oxide Nanoflowers using Surface Plasmons of Gold Nanoparticles and a Graphene Membrane. Physica Status Solidi - Rapid Research Letters, 2021, 15, 2000512.	2.4	4
38	High-performance single crystal CH3NH3PbI3 perovskite x-ray detector. Applied Physics Letters, 2021, 118, .	3.3	28
39	Filling the gap: thermal properties and device applications of graphene. Science China Information Sciences, 2021, 64, 1.	4.3	10
40	Flexible and Transparent Ultraviolet Photodetector Enabled by Metal Doping ZnO Nanorods Based on Mica Substrate. , 2021, , .		0
41	Multifunctional Graphene Microstructures Inspired by Honeycomb for Ultrahigh Performance Electromagnetic Interference Shielding and Wearable Applications. ACS Nano, 2021, 15, 8907-8918.	14.6	110
42	The manufacture and characterization of a novel ultrasonic transducer for medical imaging. , 2021, , .		1
43	A Sensitive Vertical Standing Graphene/Silicon Schottky Photodetector to Angle Changes. , 2021, , .		0
44	Compact, Flexible, and Transparent Antennas Based on Embedded Metallic Mesh for Wearable Devices in 5G Wireless Network. IEEE Transactions on Antennas and Propagation, 2021, 69, 1864-1873.	5.1	31
45	Gate-Tunable Negative Differential Resistance Behaviors in a hBN-Encapsulated BP-MoS ₂ Heterojunction. ACS Applied Materials & Interfaces, 2021, 13, 26161-26169.	8.0	21
46	The Origin of CBRAM With High Linearity, On/Off Ratio, and State Number for Neuromorphic Computing. IEEE Transactions on Electron Devices, 2021, 68, 2568-2571.	3.0	12
47	Roll-to-roll graphene films for non-disposable electrocardiogram electrodes. Journal Physics D: Applied Physics, 2021, 54, 364003.	2.8	8
48	Observation of negative capacitance in antiferroelectric PbZrO3 Films. Nature Communications, 2021, 12, 4215.	12.8	22
49	Ultrahigh Step-Up Coupled-Inductor DC-DC Converter With Soft-Switching for Driving Piezoelectric Actuators. IEEE Transactions on Circuits and Systems II: Express Briefs, 2021, 68, 2902-2906.	3.0	3
50	Reconfigurable Logic-Memory Hybrid Device Based on Ferroelectric Hf _{0.5} Zr _{0.5} O ₂ . IEEE Electron Device Letters, 2021, 42, 1164-1167.	3.9	10
51	Self-Powered Multicolor Broadband Photodetector Based on GaSe/WSeâ,,//WSeâ,,/BP Van Der Waals Heterostructure. IEEE Transactions on Electron Devices, 2021, 68, 3881-3886.	3.0	1
52	Black phosphorus junctions and their electrical and optoelectronic applications. Journal of Semiconductors, 2021, 42, 081001.	3.7	22
53	An Integrated Luminescent Information Encryption–Decryption and Anticounterfeiting Chip Based on Laser Induced Graphene. Advanced Functional Materials, 2021, 31, 2103255.	14.9	21
54	Reconfigurable MoTe ₂ Field-Effect Transistors and its Application in Compact CMOS Circuits. IEEE Transactions on Electron Devices, 2021, 68, 4748-4753.	3.0	9

#	Article	IF	CITATIONS
55	Fabricating In-Plane MoTe ₂ p-n Homojunction Photodetector Using Laser-Induced p-Type Doping. IEEE Transactions on Electron Devices, 2021, 68, 4485-4490.	3.0	3
56	Ambipolar transport compact models for two-dimensional materials based field-effect transistors. Tsinghua Science and Technology, 2021, 26, 574-591.	6.1	3
57	Transistor Subthreshold Swing Lowered by 2-D Heterostructures. IEEE Transactions on Electron Devices, 2021, 68, 411-414.	3.0	1
58	A 10Ânm Short Channel MoS ₂ Transistor without the Resolution Requirement of Photolithography. Advanced Electronic Materials, 2021, 7, 2100543.	5.1	9
59	Graphene-Based Multifunctional Textile for Sensing and Actuating. ACS Nano, 2021, 15, 17738-17747.	14.6	57
60	Hippocampal Neurons' Alignment on Quartz Grooves and Parylene Cues on Quartz Substrate. Applied Sciences (Switzerland), 2021, 11, 275.	2.5	5
61	Interfacial Regulation of Dielectric Properties in Ferroelectric Hf _{0.5} Zr _{0.5} O ₂ Thin Films. IEEE Journal of the Electron Devices Society, 2021, 9, 1093-1097.	2.1	2
62	Large Coercive Field in Hf0.5Zr0.5O2-based Capacitors with Gd Top Electrode. , 2021, , .		0
63	Ferroelectric structural transition in hafnium oxide induced by charged oxygen vacancies. Physical Review B, 2021, 104, .	3.2	35
64	Ultrasensitive Detection of COVID-19 Causative Virus (SARS-CoV-2) Spike Protein Using Laser Induced Graphene Field-Effect Transistor. Molecules, 2021, 26, 6947.	3.8	22
65	Programmable Sensitivity Screening of Strain Sensors by Local Electrical and Mechanical Properties Coupling. ACS Nano, 2021, 15, 20590-20599.	14.6	13
66	A review on low-dimensional novel optoelectronic devices based on carbon nanotubes. AIP Advances, 2021, 11, .	1.3	4
67	Modeling of Gate Tunable Synaptic Device for Neuromorphic Applications. Frontiers in Physics, 2021, 9, .	2.1	2
68	Multifunctional and high-performance electronic skin based on silver nanowires bridging graphene. Carbon, 2020, 156, 253-260.	10.3	67
69	Grapheneâ€Based Devices for Thermal Energy Conversion and Utilization. Advanced Functional Materials, 2020, 30, 1903888.	14.9	30
70	Wearable Electronics Based on 2D Materials for Human Physiological Information Detection. Small, 2020, 16, e1901124.	10.0	97
71	High-Quality Single Crystal Perovskite for Highly Sensitive X-Ray Detector. IEEE Electron Device Letters, 2020, 41, 256-259.	3.9	36
72	Fabricating Molybdenum Disulfide Memristors. ACS Applied Electronic Materials, 2020, 2, 346-370.	4.3	27

#	Article	IF	CITATIONS
73	Substrate-Free Multilayer Graphene Electronic Skin for Intelligent Diagnosis. ACS Applied Materials & Interfaces, 2020, 12, 49945-49956.	8.0	43
74	Triode-Mimicking Graphene Pressure Sensor with Positive Resistance Variation for Physiology and Motion Monitoring. ACS Nano, 2020, 14, 10104-10114.	14.6	180
75	Flexible Quasiâ€van der Waals Ferroelectric Hafniumâ€Based Oxide for Integrated Highâ€Performance Nonvolatile Memory. Advanced Science, 2020, 7, 2001266.	11.2	32
76	Anomalous thermoacoustic effect in topological insulator for sound applications. Applied Physics Letters, 2020, 117, 123502.	3.3	2
77	A Miniaturized Integrated SAW Sensing System for Relative Humidity Based on Graphene Oxide Film. IEEE Sensors Journal, 2020, 20, 9733-9739.	4.7	16
78	Fabrication and Characterization of Ferroelectric HfZrO-based Synaptic Transistors with Multi-state Plasticity. , 2020, , .		6
79	High Performance and Wireless Graphene Earphone towards Practical Applications. , 2020, , .		1
80	Encapsulated X-Ray Detector Enabled by All-Inorganic Lead-Free Perovskite Film With High Sensitivity and Low Detection Limit. IEEE Transactions on Electron Devices, 2020, 67, 3191-3198.	3.0	40
81	Graphene muscle with artificial intelligence. , 2020, , .		1
82	Fabrication and Characterization of a Novel Si Line Tunneling TFET With High Drive Current. IEEE Journal of the Electron Devices Society, 2020, 8, 336-340.	2.1	28
83	Graphene-Based Thermoacoustic Sound Source. ACS Nano, 2020, 14, 3779-3804.	14.6	33
84	A Spectrum-Tunable and Flexible Light-Emitting Device with Ultra-Wide Wavelength Range. , 2020, , .		0
85	Lower Power, Better Uniformity, and Stability CBRAM Enabled by Graphene Nanohole Interface Engineering. IEEE Transactions on Electron Devices, 2020, 67, 984-988.	3.0	9
86	Thermal Energy Conversion: Grapheneâ€Based Devices for Thermal Energy Conversion and Utilization (Adv. Funct. Mater. 8/2020). Advanced Functional Materials, 2020, 30, 2070052.	14.9	0
87	Utilization of Synergistic Effect of Dimensionâ€Differentiated Hierarchical Nanomaterials for Transparent and Flexible Wireless Communicational Elements. Advanced Materials Technologies, 2020, 5, 1901057.	5.8	4
88	Ultrafast Photodetector by Integrating Perovskite Directly on Silicon Wafer. ACS Nano, 2020, 14, 2860-2868.	14.6	86
89	Highly Sensitive, Wide-Range, and Flexible Pressure Sensor Based on Honeycomb-Like Graphene Network. IEEE Transactions on Electron Devices, 2020, 67, 2153-2156.	3.0	20
90	Highly Transparent and Sensitive Graphene Sensors for Continuous and Non-invasive Intraocular Pressure Monitoring. ACS Applied Materials & Interfaces, 2020, 12, 18375-18384.	8.0	40

#	Article	IF	CITATIONS
91	Wearable Electronics: Wearable Electronics Based on 2D Materials for Human Physiological Information Detection (Small 15/2020). Small, 2020, 16, 2070083.	10.0	4
92	Progress of Lead-Free Halide Perovskite X-ray Detectors. , 2020, , .		0
93	Selfâ€Powered MoS ₂ –PDPP3T Heterotransistorâ€Based Broadband Photodetectors. Advanced Electronic Materials, 2019, 5, 1800580.	5.1	35
94	High sensitive surface-acoustic-wave optical sensor based on two-dimensional perovskite. , 2019, , .		2
95	Miniaturized and High Precision Monitoring System for Natural Waters Using a Microflow Analyzer. , 2019, , .		0
96	Stable InSe transistors with high-field effect mobility for reliable nerve signal sensing. Npj 2D Materials and Applications, 2019, 3, .	7.9	31
97	Graphene-based Wearable Sensors for Physiological Signal Monitoring. , 2019, , .		0
98	A Wearable Skinlike Ultra-Sensitive Artificial Graphene Throat. ACS Nano, 2019, 13, 8639-8647.	14.6	80
99	A novel thermal acoustic device based on vertical graphene film. AIP Advances, 2019, 9, 075302.	1.3	10
100	Light-Enhanced Ion Migration in Two-Dimensional Perovskite Single Crystals Revealed in Carbon Nanotubes/Two-Dimensional Perovskite Heterostructure and Its Photomemory Application. ACS Central Science, 2019, 5, 1857-1865.	11.3	45
101	Plasmonâ€Enhanced InGaZnO Ultraviolet Photodetectors Tuned by Ferroelectric HfZrO. Advanced Electronic Materials, 2019, 5, 1900588.	5.1	13
102	Dualâ€Functional Nonvolatile and Volatile Memory in Resistively Switching Indium Tin Oxide/HfO <i>x</i> Devices. Physica Status Solidi (A) Applications and Materials Science, 2019, 216, 1900555.	1.8	2
103	Graphene-based wearable sensors. Nanoscale, 2019, 11, 18923-18945.	5.6	98
104	Graphene based Wearable Sensors for Healthcare. , 2019, , .		4
105	Flexible Two-Dimensional Ti ₃ C ₂ MXene Films as Thermoacoustic Devices. ACS Nano, 2019, 13, 12613-12620.	14.6	53
106	Ultra-High Sensitive NO ₂ Gas Sensor Based on Tunable Polarity Transport in CVD-WS ₂ /IGZO p-N Heterojunction. ACS Applied Materials & Interfaces, 2019, 11, 40850-40859.	8.0	105
107	Two-Mode MoS ₂ Filament Transistor with Extremely Low Subthreshold Swing and Record High On/Off Ratio. ACS Nano, 2019, 13, 2205-2212.	14.6	22
108	Tunable electronic and optical properties of the WS ₂ /IGZO heterostructure <i>via</i> an external electric field and strain: a theoretical study. Physical Chemistry Chemical Physics, 2019, 21, 14713-14721.	2.8	4

#	Article	IF	CITATIONS
109	Laser-reconfigured MoS2/ZnO van der Waals synapse. Nanoscale, 2019, 11, 11114-11120.	5.6	13
110	Photoelectric Synaptic Plasticity Realized by 2D Perovskite. Advanced Functional Materials, 2019, 29, 1902538.	14.9	132
111	X-Ray Detector Based on All-Inorganic Lead-Free Cs ₂ AgBiBr ₆ Perovskite Single Crystal. IEEE Transactions on Electron Devices, 2019, 66, 2224-2229.	3.0	57
112	Switching dynamics of ferroelectric HfO2-ZrO2 with various ZrO2 contents. Applied Physics Letters, 2019, 114, .	3.3	42
113	Simultaneous synthesis and integration of two-dimensional electronic components. Nature Electronics, 2019, 2, 164-170.	26.0	95
114	Negative Capacitance Oxide Thin-Film Transistor With Sub-60 mV/Decade Subthreshold Swing. IEEE Electron Device Letters, 2019, 40, 826-829.	3.9	26
115	Development of a portable setup using a miniaturized and high precision colorimeter for the estimation of phosphate in natural water. Analytica Chimica Acta, 2019, 1058, 70-79.	5.4	13
116	A contact lens promising for non-invasive continuous intraocular pressure monitoring. RSC Advances, 2019, 9, 5076-5082.	3.6	29
117	Scalable Modeling for the Coplanar Waveguide Step Discontinuity at Frequency up to 150 GHz. , 2019, , .		0
118	An efficient flexible graphene-based light-emitting device. Nanoscale Advances, 2019, 1, 4745-4754.	4.6	22
119	Au Nanoparticles-Decorated Surface Plasmon Enhanced ZnO Nanorods Ultraviolet Photodetector on Flexible Transparent Mica Substrate. IEEE Journal of the Electron Devices Society, 2019, 7, 196-202.	2.1	18
120	Negative Capacitance Black Phosphorus Transistors With Low SS. IEEE Transactions on Electron Devices, 2019, 66, 1579-1583.	3.0	15
121	Proton Conductor Gated Synaptic Transistor Based on Transparent IGZO for Realizing Electrical and UV Light Stimulus. IEEE Journal of the Electron Devices Society, 2019, 7, 38-45.	2.1	24
122	A Hybrid Phototransistor Neuromorphic Synapse. IEEE Journal of the Electron Devices Society, 2019, 7, 13-17.	2.1	14
123	Design and Characterization of High-Density Ultrasonic Transducer Array. IEEE Sensors Journal, 2018, 18, 2285-2290.	4.7	15
124	Graphene devices based on laser scribing technology. Japanese Journal of Applied Physics, 2018, 57, 04FA01.	1.5	19
125	Demonstration of α-InGaZnO TFT Nonvolatile Memory Using TiAlO Charge Trapping Layer. IEEE Nanotechnology Magazine, 2018, 17, 1089-1093.	2.0	8
126	All-Inorganic Perovskite Nanowires–InGaZnO Heterojunction for High-Performance Ultraviolet–Visible Photodetectors. ACS Applied Materials & Interfaces, 2018, 10, 7231-7238.	8.0	53

#	Article	IF	CITATIONS
127	Total-Ionizing-Dose Effects on a Graphene X-Ray Detector Laser-Scribed From Graphene Oxide. IEEE Transactions on Nuclear Science, 2018, 65, 473-477.	2.0	2
128	Epidermis Microstructure Inspired Graphene Pressure Sensor with Random Distributed Spinosum for High Sensitivity and Large Linearity. ACS Nano, 2018, 12, 2346-2354.	14.6	579
129	Simultaneously Detecting Subtle and Intensive Human Motions Based on a Silver Nanoparticles Bridged Graphene Strain Sensor. ACS Applied Materials & Interfaces, 2018, 10, 3948-3954.	8.0	118
130	Controlled Growth of Bilayerâ€MoS ₂ Films and MoS ₂ â€Based Fieldâ€Effect Transistor (FET) Performance Optimization. Advanced Electronic Materials, 2018, 4, 1700524.	5.1	29
131	Hybrid graphene/cadmium-free ZnSe/ZnS quantum dots phototransistors for UV detection. Scientific Reports, 2018, 8, 5107.	3.3	21
132	A Grapheneâ€Based Filament Transistor with Subâ€10 mVdec ^{â^'1} Subthreshold Swing. Advanced Electronic Materials, 2018, 4, 1700608.	5.1	21
133	Locally hydrazine doped WSe ₂ p-n junction toward high-performance photodetectors. Nanotechnology, 2018, 29, 015203.	2.6	36
134	A novel cell-scale bio-nanogenerator based on electron–ion interaction for fast light power conversion. Nanoscale, 2018, 10, 526-532.	5.6	10
135	Interface Engineering with MoS ₂ –Pd Nanoparticles Hybrid Structure for a Low Voltage Resistive Switching Memory. Small, 2018, 14, 1702525.	10.0	52
136	Heterostructured graphene quantum dot/WSe2/Si photodetector with suppressed dark current and improved detectivity. Nano Research, 2018, 11, 3233-3243.	10.4	67
137	Ultra-sensitive and plasmon-tunable graphene photodetectors for micro-spectrometry. Nanoscale, 2018, 10, 20013-20019.	5.6	34
138	Ink-injected dual-band antennas based on graphene flakes, carbon nanotubes and silver nanowires. RSC Advances, 2018, 8, 37534-37539.	3.6	6
139	High Performance 2D Perovskite/Graphene Optical Synapses as Artificial Eyes. , 2018, , .		21
140	First Principles Study of Memory Selectors using Heterojunctions of 2D Layered Materials. , 2018, , .		2
141	Multifunctional Mechanical Sensors for Versatile Physiological Signal Detection. ACS Applied Materials & amp; Interfaces, 2018, 10, 44173-44182.	8.0	36
142	High-Quality Reconfigurable Black Phosphorus p-n Junctions. IEEE Transactions on Electron Devices, 2018, , 1-5.	3.0	3
143	Toward an In Situ Phosphate Sensor in Natural Waters Using a Microfluidic Flow Loop Analyzer. Journal of the Electrochemical Society, 2018, 165, 8737-8745.	2.9	11
144	Gait Recognition Based on Graphene Porous Network Structure Pressure Sensors for Rehabilitation		6

Therapy. , 2018, , .

#	Article	IF	CITATIONS
145	Piezoelectric Micromachined Ultrasonic Transducers for Ultrasound Imaging. , 2018, , .		1
146	Millimeter-Scale Nonlocal Photo-Sensing Based on Single-Crystal Perovskite Photodetector. IScience, 2018, 7, 110-119.	4.1	14
147	Direct laser-patterned ultra-wideband antennae with carbon nanotubes. RSC Advances, 2018, 8, 31331-31336.	3.6	2
148	Wearable humidity sensor based on porous graphene network for respiration monitoring. Biosensors and Bioelectronics, 2018, 116, 123-129.	10.1	278
149	An ultrasensitive strain sensor with a wide strain range based on graphene armour scales. Nanoscale, 2018, 10, 11524-11530.	5.6	77
150	MoS ₂ Synaptic Transistor With Tunable Weight Profile. IEEE Transactions on Electron Devices, 2018, 65, 3543-3547.	3.0	13
151	Graphene FET Array Biosensor Based on ssDNA Aptamer for Ultrasensitive Hg2+ Detection in Environmental Pollutants. Frontiers in Chemistry, 2018, 6, 333.	3.6	46
152	A Two-terminal Electric-double-layer Synaptic Device with Short-term Plasticity. , 2018, , .		0
153	Multilayer Graphene Epidermal Electronic Skin. ACS Nano, 2018, 12, 8839-8846.	14.6	257
154	Field effect properties of single-layer MoS2(1â^'x)Se2x nanosheets produced by a one-step CVD process. Journal of Materials Science, 2018, 53, 14447-14455.	3.7	11
155	Graphene Textile Strain Sensor with Negative Resistance Variation for Human Motion Detection. ACS Nano, 2018, 12, 9134-9141.	14.6	455
156	A Review on Bacteriorhodopsin-Based Bioelectronic Devices. Sensors, 2018, 18, 1368.	3.8	47
157	An intelligent artificial throat with sound-sensing ability based on laser induced graphene. Nature Communications, 2017, 8, 14579.	12.8	396
158	Simulation and experimental verification of silicon dioxide deposition by PECVD. Modern Physics Letters B, 2017, 31, 1750055.	1.9	2
159	High-performance sound source devices based on graphene woven fabrics. Applied Physics Letters, 2017, 110, .	3.3	12
160	Low-Voltage Unipolar Inverter Based on Top-Gate Electric-Double-Layer Thin-Film Transistors Gated by Silica Proton Conductor. IEEE Electron Device Letters, 2017, 38, 875-878.	3.9	7
161	Novel Field Effect Transistor Fabrication Based on Non-Graphene 2D Materials. MRS Advances, 2017, 2, 3675-3684.	0.9	0
162	High-performance graphene-based flexible heater for wearable applications. RSC Advances, 2017, 7, 27001-27006.	3.6	91

#	Article	IF	CITATIONS
163	Self-adapted and tunable graphene strain sensors for detecting both subtle and large human motions. Nanoscale, 2017, 9, 8266-8273.	5.6	100
164	Top-Gate Electric-Double-Layer IZO-Based Synaptic Transistors for Neuron Networks. IEEE Electron Device Letters, 2017, 38, 588-591.	3.9	32
165	Long-Term Depression Mimicked in an IGZO-Based Synaptic Transistor. IEEE Electron Device Letters, 2017, 38, 191-194.	3.9	43
166	Flexible graphene sound device based on laser reduced graphene. Applied Physics Letters, 2017, 111, .	3.3	24
167	Synaptic Computation Demonstrated in a Two-Synapse Network Based on Top-Gate Electric-Double-Layer Synaptic Transistors. IEEE Electron Device Letters, 2017, 38, 1496-1499.	3.9	15
168	Efficient and Reversible Electron Doping of Semiconductor-Enriched Single-Walled Carbon Nanotubes by Using Decamethylcobaltocene. Scientific Reports, 2017, 7, 6751.	3.3	36
169	An analytical charge-sheet drain current model for monolayer transition metal dichalcogenide negative capacitance field-effect transistors. , 2017, , .		1
170	A Ferroelectric Thin Film Transistor Based on Annealing-Free HfZrO Film. IEEE Journal of the Electron Devices Society, 2017, 5, 378-383.	2.1	43
171	Large-Scale and High-Density pMUT Array Based on Isolated Sol-Gel PZT Membranes for Fingerprint Imaging. Journal of the Electrochemical Society, 2017, 164, B377-B381.	2.9	25
172	Graphene-Paper Pressure Sensor for Detecting Human Motions. ACS Nano, 2017, 11, 8790-8795.	14.6	572
173	Extremely Low Operating Current Resistive Memory Based on Exfoliated 2D Perovskite Single Crystals for Neuromorphic Computing. ACS Nano, 2017, 11, 12247-12256.	14.6	286
174	Tailoring perpendicular magnetic anisotropy with graphene oxide membranes. RSC Advances, 2017, 7, 52938-52944.	3.6	3
175	A super flexible and custom-shaped graphene heater. Nanoscale, 2017, 9, 14357-14363.	5.6	63
176	A simple way to grow large-area single-layer MoS <inf>2</inf> film by chemical vapor deposition. , 2017, , .		0
177	A power manager system with 78% efficiency for high-voltage triboelectric nanogenerators. Science China Information Sciences, 2017, 60, 1.	4.3	1
178	A Flexible 360-Degree Thermal Sound Source Based on Laser Induced Graphene. Nanomaterials, 2016, 6, 112.	4.1	18
179	A comparison of Pd and Au electrodes-based LiNbO ₃ surface acoustic wave devices. Modern Physics Letters B, 2016, 30, 1650349.	1.9	2
180	A Low Input Current and Wide Conversion Ratio Buck Regulator with 75% Efficiency for High-Voltage Triboelectric Nanogenerators. Scientific Reports, 2016, 6, 19246.	3.3	15

#	Article	IF	CITATIONS
181	High performance photodetector based on Pd-single layer MoS2 Schottky junction. Applied Physics Letters, 2016, 109, .	3.3	15
182	A novel thermal acoustic device based on porous graphene. AIP Advances, 2016, 6, .	1.3	9
183	Tunable and wearable high performance strain sensors based on laser patterned graphene flakes. , 2016, , .		1
184	A universal method to grow and etch graphene film. , 2016, , .		0
185	Flexible, Highly Sensitive, and Wearable Pressure and Strain Sensors with Graphene Porous Network Structure. ACS Applied Materials & Interfaces, 2016, 8, 26458-26462.	8.0	387
186	Wearable Strain Sensors: Carbonized Silk Fabric for Ultrastretchable, Highly Sensitive, and Wearable Strain Sensors (Adv. Mater. 31/2016). Advanced Materials, 2016, 28, 6639-6639.	21.0	17
187	Surface Acoustic Wave Devices Based on High Quality Temperature-Compensated Substrates. IEEE Electron Device Letters, 2016, 37, 1063-1066.	3.9	7
188	Tunable graphene oxide reduction and graphene patterning at room temperature on arbitrary substrates. Carbon, 2016, 109, 173-181.	10.3	38
189	Novel memory devices based on nanostructured carbon materials. , 2016, , .		0
190	High performance flexible strain sensor based on self-locked overlapping graphene sheets. Nanoscale, 2016, 8, 20090-20095.	5.6	108
191	A common-source amplifier based on single layer MoS <inf>2</inf> . , 2016, , .		0
192	Novel graphene-based resistive random access memory. , 2016, , .		0
193	Carbonized Silk Fabric for Ultrastretchable, Highly Sensitive, and Wearable Strain Sensors. Advanced Materials, 2016, 28, 6640-6648.	21.0	749
194	A point acoustic device based on aluminum nanowires. Nanoscale, 2016, 8, 5516-5525.	5.6	15
195	Electrical thermal acoustic point source based on mems technology. , 2016, , .		0
196	A miniaturized microbial fuel cell with three-dimensional graphene macroporous scaffold anode demonstrating a record power density of over 10 000 W m ^{â~'3} . Nanoscale, 2016, 8, 3539-3547	5.6	96
197	Zno field-effect transistors with lead-zirconate-titanate ferroelectric gate. Materials Research Innovations, 2015, 19, S2-181-S2-184.	2.3	4
198	Memory Devices: In Situ Tuning of Switching Window in a Gate-Controlled Bilayer Graphene-Electrode Resistive Memory Device (Adv. Mater. 47/2015). Advanced Materials, 2015, 27, 7766-7766.	21.0	1

#	Article	IF	CITATIONS
199	Flexible CNT-array double helices Strain Sensor with high stretchability for Motion Capture. Scientific Reports, 2015, 5, 15554.	3.3	55
200	In Situ Tuning of Switching Window in a Gateâ€Controlled Bilayer Grapheneâ€Electrode Resistive Memory Device. Advanced Materials, 2015, 27, 7767-7774.	21.0	54
201	Graphem stack: Growth, characterization and diverse devices. , 2015, , .		0
202	A flexible, transparent and ultrathin single-layer graphene earphone. RSC Advances, 2015, 5, 17366-17371.	3.6	39
203	Observation of a giant two-dimensional band-piezoelectric effect on biaxial-strained graphene. NPG Asia Materials, 2015, 7, e154-e154.	7.9	58
204	A Graphene-Based Resistive Pressure Sensor with Record-High Sensitivity in a Wide Pressure Range. Scientific Reports, 2015, 5, 8603.	3.3	415
205	Coherent Generation of Photo-Thermo-Acoustic Wave from Graphene Sheets. Scientific Reports, 2015, 5, 10582.	3.3	33
206	A spectrally tunable all-graphene-based flexible field-effect light-emitting device. Nature Communications, 2015, 6, 7767.	12.8	113
207	A Pressure Sensing System for Heart Rate Monitoring with Polymer-Based Pressure Sensors and An Anti-Interference Post Processing Circuit. Sensors, 2015, 15, 3224-3235.	3.8	76
208	Controllable Thermal Rectification Realized in Binary Phase Change Composites. Scientific Reports, 2015, 5, 8884.	3.3	49
209	Graphene Dynamic Synapse with Modulatable Plasticity. Nano Letters, 2015, 15, 8013-8019.	9.1	226
210	A novel MEMS-based 13.56 MHz micro antenna for RFID application. , 2015, , .		1
211	Biological information wireless monitoring system. , 2015, , .		0
212	A high performance triboelectric nanogenerator for self-powered non-volatile ferroelectric transistor memory. Nanoscale, 2015, 7, 17306-17311.	5.6	46
213	PROTON IRRADIATION INFLUENCE ON THE MAGNETIC PROPERTIES OF GMR-SVs. Modern Physics Letters B, 2014, 28, 1450022.	1.9	2
214	An ultra-sensitive resistive pressure sensor based on the V-shaped foam-like structure of laser-scribed graphene. , 2014, , .		1
215	REACTION SIMULATION AND EXPERIMENT OF A Cl ₂ / Ar INDUCTIVELY COUPLED PLASMA FOR ETCHING OF SILICON. Surface Review and Letters, 2014, 21, 1450038.	1.1	3
216	Large-scale fabrication of graphene-based electronic and MEMS devices. , 2014, , .		1

#	Article	IF	CITATIONS
217	Novel flexible nanogenerators. , 2014, , .		Ο
218	Modeling and analysis of nano-sized GMRs based on Co, NiFe and Ni materials. Science China Information Sciences, 2014, 57, 1-14.	4.3	1
219	A micro-scale microbial supercapacitor. , 2014, , .		1
220	Graphene Earphones: Entertainment for Both Humans and Animals. ACS Nano, 2014, 8, 5883-5890.	14.6	105
221	Scalable fabrication of high-performance and flexible graphene strain sensors. Nanoscale, 2014, 6, 699-705.	5.6	366
222	Growth and Raman Spectra of Single-Crystal Trilayer Graphene with Different Stacking Orientations. ACS Nano, 2014, 8, 10766-10773.	14.6	56
223	Cost-Effective, Transfer-Free, Flexible Resistive Random Access Memory Using Laser-Scribed Reduced Graphene Oxide Patterning Technology. Nano Letters, 2014, 14, 3214-3219.	9.1	114
224	Wafer-Scale Integration of Graphene-based Electronic, Optoelectronic and Electroacoustic Devices. Scientific Reports, 2014, 4, 3598.	3.3	113
225	Novel Field-Effect Schottky Barrier Transistors Based on Graphene-MoS2 Heterojunctions. Scientific Reports, 2014, 4, 5951.	3.3	134
226	Magnetoresistive behavior and magnetization reversal of NiFe/Cu/CoFe/IrMn spin valve GMRs in nanoscale. International Journal of Minerals, Metallurgy and Materials, 2013, 20, 700-704.	4.9	6
227	Flexible and large-area sound-emitting device using reduced graphene oxide. , 2013, , .		4
228	A multi-mode complex bandpass filter with gm-assisted power optimization and I/Q calibration. , 2013, , .		4
229	A reduced graphene oxide sound-emitting device: a new use for Joule heating. RSC Advances, 2013, 3, 17672.	3.6	22
230	Temperature Control of P(VDF-TrFE) Copolymer Thin Films. Integrated Ferroelectrics, 2013, 141, 187-194.	0.7	36
231	Wafer-scale flexible graphene strain sensors. , 2013, , .		1
232	Graphene/semiconductor heterojunction solar cells with modulated antireflection and graphene work function. Energy and Environmental Science, 2013, 6, 108-115.	30.8	154
233	Effects of anode materials on resistive characteristics of NiO thin films. Applied Physics Letters, 2013, 102, .	3.3	15
234	Monitoring Oxygen Movement by Raman Spectroscopy of Resistive Random Access Memory with a Graphene-Inserted Electrode. Nano Letters, 2013, 13, 651-657.	9.1	121

#	Article	IF	CITATIONS
235	Ambipolar/unipolar conversion in graphene transistors by surface doping. Applied Physics Letters, 2013, 103, 193502.	3.3	10
236	Enhanced dielectric and multiferroic properties of single-phase Y and Zr co-doped BiFeO3 ceramics. Journal of Applied Physics, 2013, 114, .	2.5	55
237	SIMULATION METHODS OF PIEZORESISTIVE PRESSURE SENSORS IN ORDER TO IMPROVE CONSISTENCY. Modern Physics Letters B, 2013, 27, 1350011.	1.9	1
238	Design of magnetic RF inductor in CMOS. Tsinghua Science and Technology, 2012, 17, 78-83.	6.1	7
239	Resistive switching behavior in diamond-like carbon films grown by pulsed laser deposition for resistance switching random access memory application. Journal of Applied Physics, 2012, 111, 084501.	2.5	31
240	ZnO nanorod array based optoelectronic device with graphene as transparent electrode. , 2012, , .		0
241	Investigation of the improved performance in a graphene/polycrystalline BiFeO3/Pt photovoltaic heterojunction: Experiment, modeling, and application. Journal of Applied Physics, 2012, 112, .	2.5	23
242	Influence of La and Mn dopants on the current-voltage characteristics of BiFeO3/ZnO heterojunction. Journal of Applied Physics, 2012, 111, .	2.5	37
243	Electrode/oxide interface engineering by inserting single-layer graphene: Application for HfO <inf>x</inf> -based resistive random access memory. , 2012, , .		12
244	Light-Induced Modulation in Resistance Switching of Carbon Nanotube/BiFeO ₃ /Pt Heterostructure. Integrated Ferroelectrics, 2012, 134, 58-64.	0.7	4
245	Optimization of graphene/silicon heterojunction solar cells. , 2012, , .		4
246	Multilayer graphene growth by a metal-catalyzed crystallization of diamond-like carbon. , 2012, , .		0
247	Comparative Study on Structural and Ferroelectric Properties of Dual-Site Rare-Earth Ions Substituted Multiferroelectric BiFeO ₃ . Integrated Ferroelectrics, 2012, 132, 30-38.	0.7	6
248	Unipolar to ambipolar conversion in graphene field-effect transistors. Applied Physics Letters, 2012, 101, .	3.3	17
249	Light-Induced Modulation in Resistance Switching of Carbon Nanotube/ BiFeO ₃ /Pt Heterostructure. Integrated Ferroelectrics, 2012, 132, 53-60.	0.7	0
250	Static behavior of a graphene-based sound-emitting device. Nanoscale, 2012, 4, 3345.	5.6	28
251	Micromachined piezoelectric devices for acoustic applications. , 2012, , .		1
252	Single-layer graphene sound-emitting devices: experiments and modeling. Nanoscale, 2012, 4, 2272.	5.6	92

#	Article	IF	CITATIONS
253	Temperature dependence of optical and structural properties of ferroelectric B3.15Nd0.85Ti3O12 thin film derived by sol–gel process. Journal of Sol-Gel Science and Technology, 2012, 61, 236-242.	2.4	6
254	Nd-doped Bismuth Titanate based ferroelectric field effect transistor: Design, fabrication, and optimization. , 2011, , .		0
255	Research for piezoresistive pressure sensors: Methods to reduce the influence of processing deviation on sensitivity and improve product consistency. , 2011, , .		0
256	Surface acoustic wave characteristics based on c-axis (006) LiNbO3/diamond/silicon layered structure. Applied Physics Letters, 2011, 99, .	3.3	14
257	Modulation Effect of Lead Zirconate Titanate for Zinc Oxide Channel Resistance in Ferroelectric Field Effect Transistor. Ferroelectrics, 2011, 421, 92-97.	0.6	5
258	Enhanced photovoltaic properties in graphene/polycrystalline BiFeO3/Pt heterojunction structure. Applied Physics Letters, 2011, 99, .	3.3	97
259	Graphene based Schottky junction solar cells on patterned silicon-pillar-array substrate. Applied Physics Letters, 2011, 99, 233505.	3.3	76
260	Transparent, flexible, ultrathin sound source devices using Indium Tin oxide films. Applied Physics Letters, 2011, 99, .	3.3	56
261	Graphene-on-Paper Sound Source Devices. ACS Nano, 2011, 5, 4878-4885.	14.6	197
262	Comparisons and analyses on heterostructures consisting of ZnO and different ferroelectric films. Materials Research Society Symposia Proceedings, 2011, 1368, 1.	0.1	2
263	Flexible, ultrathin, and transparent sound-emitting devices using silver nanowires film. Applied Physics Letters, 2011, 99, .	3.3	46
264	Poly(3,4-ethylenedioxythiophene):poly(styrenesulfonate)-based organic, ultrathin, and transparent sound-emitting device. Applied Physics Letters, 2011, 99, 233503.	3.3	24
265	Characteristics of Pt/BiFeO3/TiO2/Si capacitors with TiO2 layer formed by liquid-delivery metal organic chemical vapor deposition. Applied Physics Letters, 2010, 97, .	3.3	13
266	Study of Iridium Bottom Electrode in Ferroelectric Random Access Memory Application. Ferroelectrics, 2010, 406, 97-107.	0.6	1
267	A metrology of silicon film thermal conductivity using micro-Raman spectroscopy. , 2010, , .		3
268	Ultrasonic transducer array design for medical imaging based on MEMS technologies. , 2010, , .		11
269	Bipolar switching analysis and negative resistance phenomenon in TiO. , 2010, , .		0
270	A MEMS-based flexible electrode array using composite substrate. , 2010, , .		1

A MEMS-based flexible electrode array using composite substrate. , 2010, , . 270

#	Article	IF	CITATIONS
271	A novel fatigue-insensitive self-referenced scheme for 1T1C FRAM. , 2010, , .		3
272	Amplifier high linearization method based on offset cancellation technique. , 2009, , .		1
273	Comparison of PbZr1â^'xTixO3 thin films deposited on different substrates by liquid delivery metal organic chemical vapor deposition. Journal of Applied Physics, 2009, 105, 061611.	2.5	0
274	Optimal RF IC design based on Fuzzy Genetic Algorithm. , 2009, , .		1
275	Implantable Subdural Electrode Arrays for Neural Recordings Based on MEMS Technologies. , 2009, , .		1
276	Fabrication and Properties of \$hbox{Pt}/hbox{Bi}_{3.15}hbox{Nd}_{0.85} hbox{Ti}_{3}hbox{O}_{12}/reakhbox{HfO}_{2}/hbox{Si}\$ Structure for Ferroelectric DRAM (FEDRAM) FET. IEEE Electron Device Letters, 2009, 30, 463-465.	3.9	6
277	Structural, ferroelectric, dielectric, and magnetic properties of BiFeO3/Bi3.15Nd0.85Ti3O12 multilayer films derived by chemical solution deposition. Journal of Applied Physics, 2009, 105, 084109.	2.5	20
278	Characterization of Pt/Bi3.15Nd0.85Ti3O12/HfO2/Si structure using a hafnium oxide as buffer layer for ferroelectric-gate field effect transistors. Journal of Applied Physics, 2009, 106, .	2.5	13
279	A novel method for fabricating 2-D array piezoelectric micromachined ultrasonic transducers for medical imaging. , 2009, , .		1
280	A multi-frequency wireless passive pressure sensor for TPMS applications. , 2009, , .		2
281	Withdrawal of "Fabrication and Properties of <formula formulatype="inline"> <tex notation="TeX">\$ hbox{Pt}/hbox{Bi}_{3.15}hbox{Nd}_{0.85}hbox{Ti}_{3}hbox{O}_{12}/hbox{HfO}_{2}/hbox{Si}\$</tex> </formula> Structure for Ferroelectric DRAM (FEDRAM) FET". IEEE Electron Device Letters, 2009, 30, 1111-1111.	3.9	3
282	NOVEL DEVICE DESIGN FOR AN ULTRASONIC RANGING SYSTEM. Integrated Ferroelectrics, 2009, 105, 53-65.	0.7	8
283	A novel MEMS pressure sensor with MOSFET on chip. , 2008, , .		23
284	Modeling and analysis of effect on bit-line voltage caused by imprint in FeRAM. , 2008, , .		0
285	OPTICAL CHARACTERIZATION OF Sr1â^xBaxBi4Ti4O15 GRADED THIN FILMS. Integrated Ferroelectrics, 2008, 98, 128-135.	0.7	0
286	DEVICE DESIGN FOR THE NOVEL HANDWRITING RECOGNITION SYSTEM. Integrated Ferroelectrics, 2008, 100, 206-215.	0.7	7
287	A novel circuit scheme and analysis for three-level feram. , 2008, , .		0
288	Buffer layer dependence of B <inf>3.15</inf> Nd <inf>0.85</inf> Ti <inf>3</inf> O <inf>12</inf> (BNdT) based MFIS capacitor for FeFET application. , 2008, , .		0

#	Article	IF	CITATIONS
289	AN INNOVATED PROCESS OF Pt/PbTiO3/PbZr0.3Ti0.7O3/PbTiO3/Pt INTEGRATED FERROELECTRIC CAPACITORS FOR FeRAM. Integrated Ferroelectrics, 2007, 89, 3-11.	0.7	5
290	UNIFORMITY IMPROVEMENT OF PZT BASED ULTRASONIC TRANSDUCER. Integrated Ferroelectrics, 2006, 80, 373-381.	0.7	5
291	Measurements of Ferroelectric MEMS Microphones. Integrated Ferroelectrics, 2005, 69, 417-429.	0.7	4
292	Key Integration Techniques and Issues for Silicon-Based Ferroelectric Devices. Integrated Ferroelectrics, 2004, 66, 59-69.	0.7	1
293	A novel ferroelectric based microphone. Microelectronic Engineering, 2003, 66, 683-687.	2.4	9
294	Piezoelectric and ferroelectric films for microelectronic applications. Materials Science and Engineering B: Solid-State Materials for Advanced Technology, 2003, 99, 159-163.	3.5	27
295	Studies of a PT/PZT/PT sandwich structure for feram applications using sol-gel processing. Integrated Ferroelectrics, 2001, 39, 215-222.	0.7	4
296	Introductory Chapter: Perovskite Materials and Advanced Applications. , 0, , .		0
297	Anisotropic electrical properties of aligned PtSe2 nanoribbon arrays grown by a pre-patterned selenization process. Nano Research, 0, , 1.	10.4	1